Semimechanistic Pharmacodynamic Modeling of Aztreonam-Avibactam Combination to Understand Its Antimicrobial Activity Against Multidrug-Resistant Gram-Negative Bacteria

Alexia Chauzy, Bruna Gaelzer Silva Torres, Julien Buyck, Boudewijn Jonge, Christophe Adier, Sandrine Marchand, William Couet, Nicolas Grégoire

Citation: CPT Pharmacometrics Syst. Pharmacol. (2019) 8, 815–824; doi:10.1002/psp4.12452

ARTICLE

Semimechanistic Pharmacodynamic Modeling of Aztreonam-Avibactam Combination to Understand Its Antimicrobial Activity Against Multidrug-Resistant Gram-Negative Bacteria

Alexia Chauzy[1,2,†], Bruna Gaelzer Silva Torres[1,2,†], Julien Buyck[1,2], Boudewijn de Jonge[3], Christophe Adier[1,4], Sandrine Marchand[1,2,4], William Couet[1,2,4,*] and Nicolas Grégoire[1,2]

Aztreonam-avibactam (ATM-AVI) is a promising combination to treat serious infections caused by multidrug-resistant (MDR) pathogens. Three distinct mechanisms of action have been previously characterized for AVI: inhibition of ATM degradation by β-lactamases, proper bactericidal effect, and enhancement of ATM bactericidal activity. The aim of this study was to quantify the individual contribution of each of the three AVI effects. *In vitro* static time-kill studies were performed on four MDR *Enterobacteriaceae* with different β-lactamase profiles. β-Lactamase activity was characterized by measuring ATM concentrations over 27 hours. Data were analyzed by a semimechanistic pharmacodynamics modeling approach. Surprisingly, even though AVI prevented ATM degradation, the combined bactericidal activity was mostly explained by the enhancement of ATM effect within clinical range of ATM (5–125 mg/L) and AVI concentrations (0.9–22.5 mg/L). Therefore, when selecting a β-lactamase inhibitor for combination with a β-lactam, its capability to enhance the β-lactam activity should be considered in addition to the spectrum of β-lactamases inhibited.

Study Highlights

WHAT IS THE CURRENT KNOWLEDGE ON THE TOPIC?
☑ Three distinct effects have been previously characterized for avibactam (AVI): inhibition of aztreonam (ATM) degradation by β-lactamases, proper bactericidal effect, and enhancement of ATM bactericidal activity.

WHAT QUESTION DID THIS STUDY ADDRESS?
☑ What is the individual contribution of each of the three AVI effects on the combined bactericidal activity with ATM?

WHAT DOES THIS STUDY ADD TO OUR KNOWLEDGE?
☑ The combined bactericidal activity was mostly explained by the enhancement of ATM effect by AVI, whereas the inhibition of β-lactamases by AVI poorly contributed to the total effect.

HOW MIGHT THIS CHANGE DRUG DISCOVERY, DEVELOPMENT, AND/OR THERAPEUTICS?
☑ Decisions on suitable dosing regimens for ATM-AVI combination in particular and, more generally, for any β-lactam/β-lactamase inhibitor combination should be made considering if the β-lactamase inhibitor is able or not to enhance β-lactam activity and not only the spectrum of β-lactamases inhibited by β-lactamase inhibitor.

Aztreonam-avibactam (ATM-AVI) is a promising combination intended to treat serious infections caused by multidrug-resistant (MDR) pathogens, in particular those producing metallo-β-lactamases (MBLs). AVI is a new and potent inhibitor of β-lactamases of Ambler classes A and C, including serine-based carbapenemases, and some class D, but it does not inhibit class B MBLs. However, in combination with ATM, a monobactam antibiotic, which is not hydrolyzed by MBLs, AVI can restore the ATM antibiotic activity against strains that produce a broad range of β-lactamases.[1]

β-Lactamase inhibitors belonging to the diazabicyclooctane (DBO) class, of which AVI is a representative, can show different types of activities.[2] These compounds are able to covalently bind to serine residues at the active site of a variety of β-lactamases causing enzyme inhibition. They can also have a direct antibacterial activity mainly due to the

[†]These authors contributed equally to this work.

[1]INSERM, U1070, Pôle Biologie Santé, Poitiers Cedex 9, France; [2]Université de Poitiers, UFR de Médecine Pharmacie, Poitiers, France; [3]Pfizer Essential Health, Cambridge, Massachusetts, USA; [4]Laboratoire de Toxicologie-Pharmacocinétique, CHU de Poitiers, Poitiers, France. *Correspondence: William Couet (william.couet@univ-poitiers.fr)

Received: May 10, 2019; accepted: June 17, 2019. doi:10.1002/psp4.12452

*inhibition of penicillin-binding proteins 2 (PBP2)[3] and can act as an enhancer when combined with β-lactam agents that bind to other PBPs.

To better understand the complex pharmacodynamics (PDs) of ATM-AVI combination, a semimechanistic model–derived from constant-concentration time-kill experiments–was developed by Sy *et al*.[4] for MDR *Enterobacteriaceae* (*Escherichia coli* and *Klebsiella pneumonia*) and *Pseudomonas aeruginosa* strains. The model considered the intrinsic bactericidal activities of ATM and AVI, degradation of ATM due to β-lactamases, and inhibition of ATM degradation due to AVI. Additionally, a synergistic function characterizing the ability of AVI to enhance ATM activity was implemented into the model. The same approach was used to characterize the activity of ceftazidime in combination with AVI for *P. aeruginosa* strains.[5]

This study aimed to further investigate the individual contribution of each of the three AVI PD effects[3,6] with the following steps: first, extend the semimechanistic PD model previously described[4] with four additional MDR *Enterobacteriaceae* isolates (representing two additional species), and, thereafter, quantify the impact of each AVI effect by simulating these effects separately in response to clinical ATM and AVI concentrations.

METHODS

Chemicals

ATM was purchased from Sigma-Aldrich, St. Quentin Fallavier, France. AVI was supplied by Pfizer, New York, NY. Stock solutions of 50 mg/mL of ATM in methanol/dimethyl sulfoxide (50/50, v/v) and 1 mg/mL of AVI in sterile water were prepared and frozen at −80°C. The stock solutions were diluted in cation-adjusted Mueller-Hinton broth on the day of experiment to achieve the desired concentrations used in the static time-kill studies.

Bacterial strains

Four MDR *Enterobacteriaceae* were obtained from International Health Management Associates Laboratory (International Health Management Associates, Schaumburg, IL). All isolates investigated in the present study produced multiple β-lactamases as follows: *E. coli* 1266865 (TEM-OSBL(b), CMY-42, and NDM-5), *Citrobacter freundii* 974673 (SHV-12(2be), TEM-OSBL(2b), CTX-M-3, CMY-34, and NDM-1), *Enterobacter cloacae* 1285905 (CTX-M-15 and NDM-1), and *E. cloacae* 1318536 (CTX-M-15 and NDM-1). Bacteria were stored at −80°C and subcultured in Mueller-Hinton agar plates (bioMérieux, Marcy-l'Etoile, France) for 24 hours at 37°C prior to each experiment.

In vitro strain susceptibility

For each strain, ATM minimum inhibitory concentrations (MICs) were determined in the absence and in the presence of AVI (0.004–4 mg/L, in twofold increments), according to EUCAST broth microdilution method.[7] The MICs of AVI without ATM were also determined for the four strains.

Static time-kill studies

The *in vitro* constant-concentration time-kill studies included a growth control, AVI alone, ATM alone, and ATM-AVI combinations. The concentrations of ATM alone and in combination were based on its respective MIC values at selected AVI concentrations (ranging from 0–8 mg/L), consisting of 0.25–4 times the MIC in twofold increment.[8] In the experiments performed with AVI as monotherapy, AVI concentrations were chosen to cover the concentrations used in combination plus onefold and twofold its MIC, ranging from 0.004–64 mg/L. In sum, 32 static time-kill assays were conducted for each strain, including 1 control, 6 levels of AVI alone, 5 levels of ATM alone, and 20 ATM-AVI combinations.

On the day of experiment, bacteria inoculum was prepared in sterile saline solution by adjusting the turbidity to a McFarland value of 0.5 corresponding to ~1.5×10^8 cfu/mL. Then, 200 μL of the bacterial suspension was added to 20 mL of cation-adjusted Mueller-Hinton broth containing different ATM and AVI concentrations, as described above, achieving a final bacterial density of 1.5×10^6 cfu/mL. The flasks were incubated at 37°C with shaking (150 rpm), and samples were collected up to 27 hours (at times 0, 2, 4, 6, 8, 10, 15, 21, 24, and 27 hours). The samples were diluted in 100-fold increments in sterile water, and 100 μL of each dilution and also undiluted samples were spread on Mueller-Hinton agar plates using an automatic diluter and plater (easySpiral Pro; Interscience, Saint-Nom-la-Bretèche, France). Bacterial colonies were counted using an automatic colony counter (Scan 300; Interscience, Saint-Nom-la-Bretèche, France) after 16–18 hours of incubation at 37°C. The lower limit of bacterial colony quantification was 200 cfu/mL. All experiments were performed at least in duplicate on separate occasions.

The presence of less-susceptible subpopulations of bacteria was assessed by plating an initial inoculum of 10^8 cfu/mL onto agar plates supplemented with ATM-AVI at concentrations of 1–16 times the ATM MIC in combination.

Drug stability analysis

Actual concentrations of ATM and AVI in the media during the time-kill experiments were measured by liquid chromatography tandem mass spectrometry (**Supplementary Material S1**) in order to monitor ATM and AVI degradation. Samples collected for bacterial counts at times 0, 8, 15, and 24 hours were centrifuged (14,000*g* for 5 minutes), and supernatants were stored at −80°C until assay. For the experiments performed with ATM alone, all samples collected during time-kill studies were used for drug quantification because a higher degradation rate was expected in the absence of AVI.

PD model

The previous semimechanistic model developed by Sy *et al*.[4] was applied to the time-kill studies data—bacterial counts and drug concentrations—and slightly modified to describe bacterial response to ATM-AVI combinations and ATM degradation for the additional studied strains.

The model was developed using NONMEM 7.4 in two steps: first, bacterial counts were fitted assuming no drug degradation; then, parameters related to bacterial response were fixed, and drug concentrations data were included in the data set to estimate the parameters for ATM degradation

and inhibition by AVI. In the final model, parameters for both bacteria and drug data were estimated simultaneously. The detailed explanation of the *in vitro* PD model is available in the **Supplementary Material**.

Simulations

Simulations using the final model (full model) were conducted to predict bacterial counts in response to a constant concentration of 25 mg/L of ATM and 4.5 mg/L of AVI, mimicking the average concentrations (C_{avg}) achieved in humans after administration every 8 hours of 2 g ATM alone[9] and 0.5 g AVI in combination with ceftazidime.[10] ATM degradation and its inhibition by AVI were also predicted. Additionally, the final model was reduced by keeping the parameters related to only one AVI effect each time—β-lactamase inhibition, bactericidal activity, or enhancement of β-lactam activity—and new simulations were conducted in order to evaluate the individual contribution of each AVI effect. A detailed procedure of how the full model was reduced is described in the **Supplementary Material**. Simulations using a model maintaining only the parameters related to ATM bactericidal effect were also performed for comparison purposes. For all additional simulations, the same constant average concentrations were used. Moreover, the way that clinically observed range of ATM-AVI concentrations impacts AVI effects was investigated. Complementary simulations were carried at high (125 and 22.5 mg/L for ATM and AVI, respectively) and low (5 and 0.9 mg/L for ATM and AVI, respectively) concentration levels using the final and the reduced models. The high levels were close to peak concentrations (C_{max}) and the low levels to concentrations achieved during the elimination phase after administration of 2 *g* ATM and 0.5 *g* AVI every 8 hours.[9,10] The area under each simulated $\log_{10}$ colony-forming unit (CFU)-time curve (AUC_{CFU}) was then determined. The maximum effect of the combination for each concentration level was defined as the difference between the AUC_{CFU} of the control ($AUC_{CFU,control}$, with no drug) and the AUC_{CFU} when all effects (ATM effect + the three AVI effects) were taken into account ($AUC_{CFU,full}$). The percentage of the maximum effect induced by each AVI effect was then calculated, as follows:

$$\%\ \text{maximum effect} = \frac{(AUC_{CFU,control} - AUC_{CFU,i})}{(AUC_{CFU,control} - AUC_{CFU,full})} \times 100$$

Where *i* corresponded to the AVI effect considered.

RESULTS

In vitro strains susceptibility

MICs of ATM in the absence and presence of 4 mg/L of AVI and MICs of AVI alone are presented in **Table 1** for the four strains studied. All strains were resistant to ATM alone resulting in elevated MIC values (between 32 and 512 mg/L). AVI restored the susceptibility of all strains to ATM according to the EUCAST resistant breakpoint of ATM for *Enterobacteriaceae* (>4 mg/L),[11] although the impact of AVI on *E. coli* strain was much less pronounced than on the others. AVI showed some, while limited, intrinsic antimicrobial activity with MIC values of 16 and 32 mg/L.

Table 1 Susceptibility and β-lactamase content of the MDR strains

Strain	β-lactamases	MIC (mg/L)		
		ATM	ATM-AVI[a]	AVI
Escherichia coli 1266865	NDM-5, TEM-OSBL(b), CMY-42	32	4	16
Citrobacter freundii 974673	NDM-1, SHV-12(2be), TEM-OSBL(2b), CTX-M-3, CMY-34	512	0.125	16
Enterobacter cloacae 1285905	NDM-1, CTX-M-15	64	0.25	32
Enterobacter cloacae 1318536	NDM-1, CTX-M-15	512	0.125	16

ATM, aztreonam; AVI, avibactam; MDR, multidrug resistant; MIC, minimum inhibitory concentration.
[a]AVI at 4 mg/L.

Static time-kill studies and drug stability

The static time-kill profiles and ATM degradation are partly shown in representative **Figures 1 and 2** for *E. coli* 1266865 and *E. cloacae* 1285905. Complete profiles containing all ATM-AVI combinations tested for the four strains are shown in **Supplementary Material** (**Figures S1–S4**). Top panels represent bacterial counts over time, and bottom panels show the corresponding percentage of ATM remaining in the system.

In the experiments performed with ATM alone (**Figures 1 and 2, top panels a**), for all studied strains, an increase in ATM concentrations resulted in an increase in bacterial killing. Except for *E. coli* 1266865 (**Figure 1, bottom panels a**), ATM degradation was observed for all the other strains when ATM concentrations were not sufficient to decrease bacterial counts from the initial inoculum (**Figure 2, bottom panels a**). ATM degradation was, thus, dependent on bacterial counts and visual observation of curves suggested that ATM degradation was rapid when bacteria reached ~10^7 cfu/mL, consistent with previous results.[12]

AVI alone had bactericidal activity against all strains at concentration levels of onefold and twofold the MIC (**Figures 1 and 2, top panels b**), and no relevant AVI degradation was observed (data not shown).

In combination, an increase in bacterial susceptibility to ATM was observed resulting from increasing concentrations of AVI; therefore, at the same ATM level, different bactericidal activity was observed according to AVI concentrations (**Figures 1 and 2, top panels c**). In addition, the rate and extent of ATM degradation was also related to AVI concentrations because AVI could prevent ATM degradation in a concentration-dependent manner starting at very low AVI concentrations, such as 0.004 mg/L (**Figure 2, bottom panels c**). By contrast, in *E. coli* 1266865, in which no relevant ATM degradation was observed even in the absence of AVI (**Figure 1, bottom panels**), an increase of ATM bactericidal activity related to AVI concentration was still observed (**Figure 1, top panels c**).

PD model

The schematic representation of the refined model that characterized the bacterial response of these four

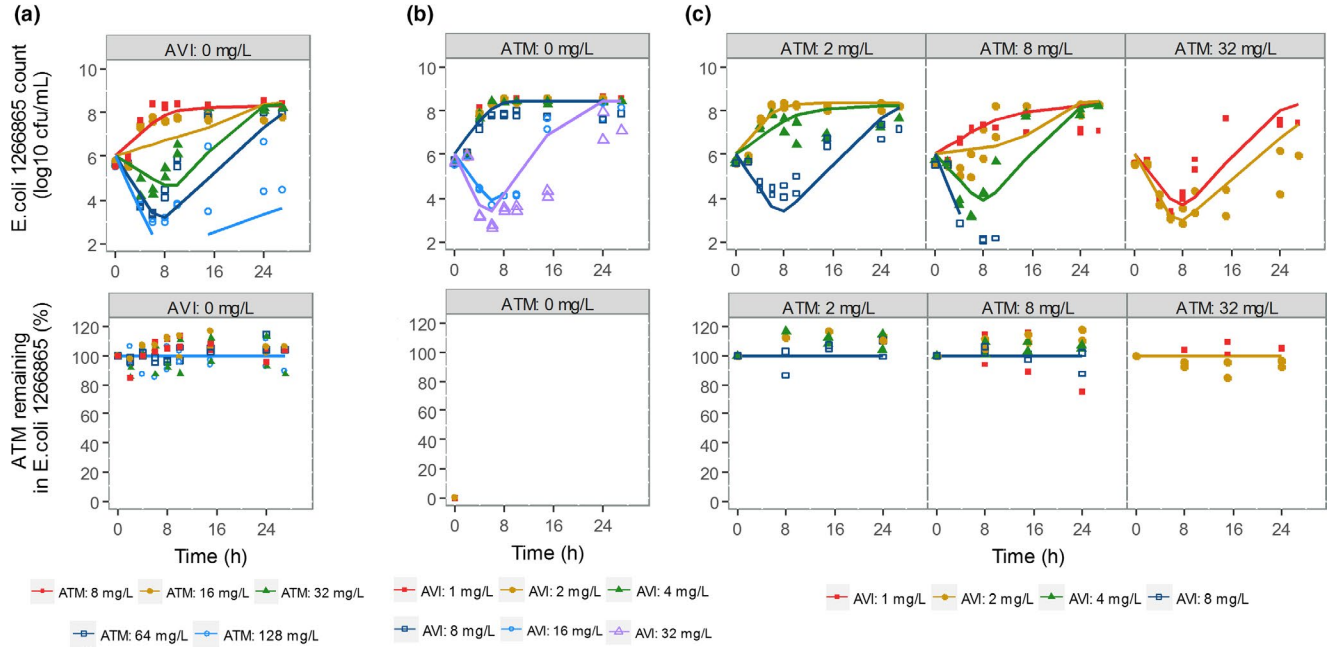

Figure 1 Model-prediction and observed static time-kill curves of (**a**) ATM alone, (**b**) AVI alone, and (**c**) ATM-AVI in combination against *Escherichia coli* 1266865 over 27 hours (top panels) and the percentage of the initial ATM concentration remaining in the system during the time-kill experiments (bottom panels). The symbols represent the experimental data (n = 2) and the color-matched lines the predictions from the pharmacodynamic model. ATM, aztreonam; AVI, avibactam.

additional studied strains to ATM-AVI combination is illustrated in **Figure 3**, and model parameter estimates are summarized in **Table 2**. The semimechanistic PD model presented here described reasonably well the growth and death of the four strains in response to ATM and AVI, as well as the bacteria-mediated ATM degradation and the inhibition of ATM degradation by AVI, as shown in **Figures 1, 2 and Figures S1–S4**.

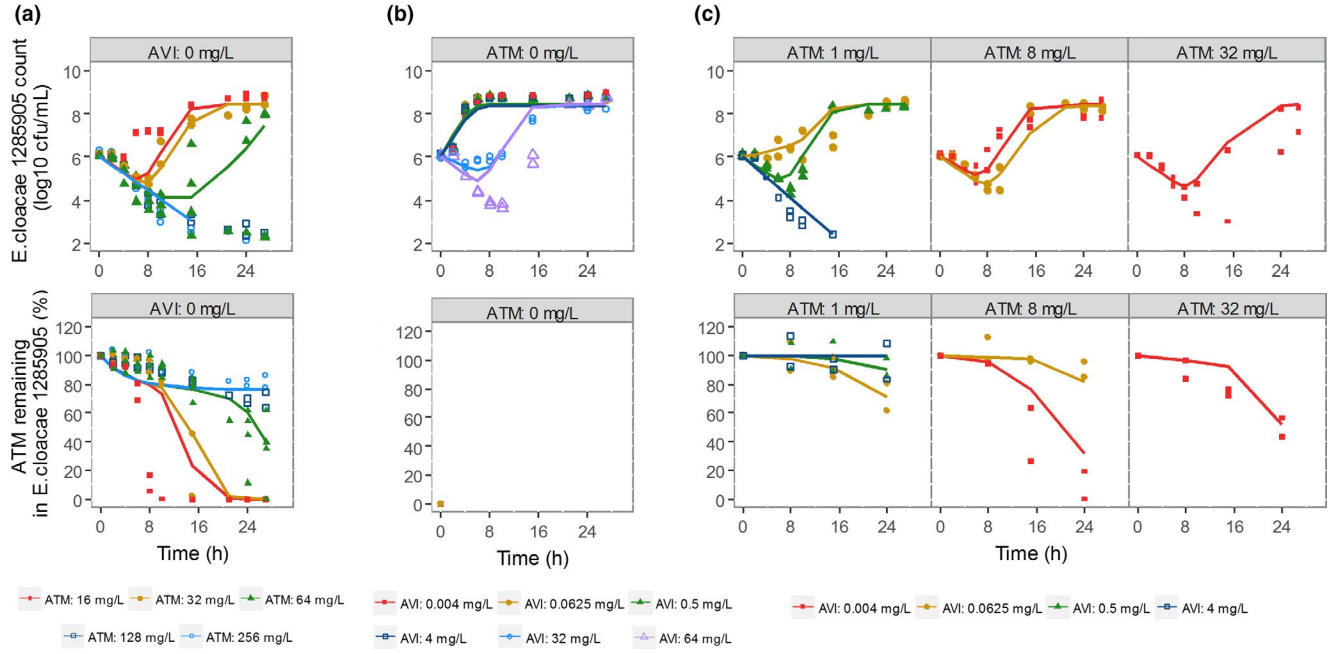

Figure 2 Model-prediction and observed static time-kill curves of (**a**) ATM alone, (**b**) AVI alone, and (**c**) ATM-AVI in combination against *Enterobacter cloacae* 1285905 over 27 hours (top panels) and the percentage of the initial ATM concentration remaining in the system during the time-kill experiments (bottom panels). The symbols represent the experimental data (n = 2) and the color-matched lines the predictions from the pharmacodynamic model. ATM, aztreonam; AVI, avibactam.

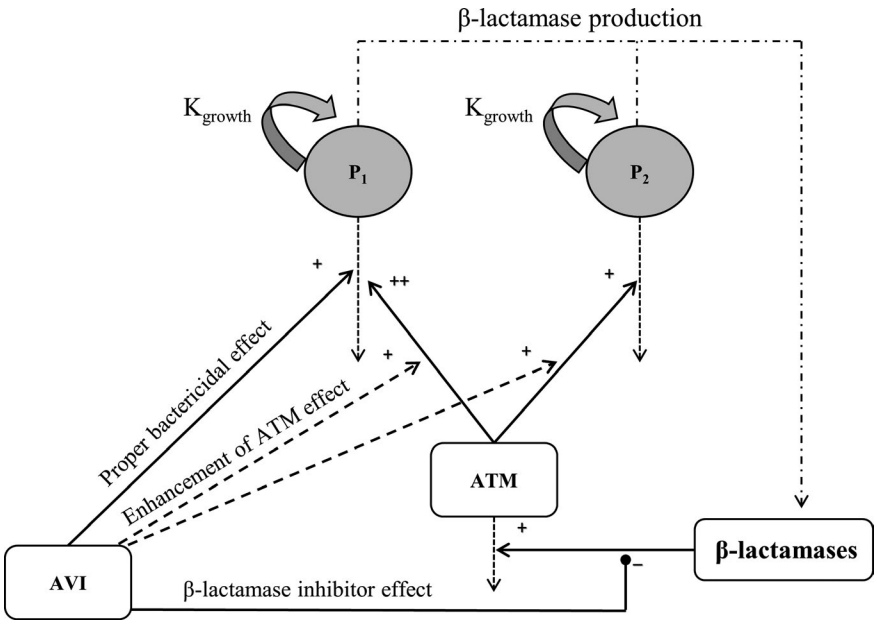

Figure 3 Schematic representation of the final model used to characterize ATM-AVI killing effect on drug-susceptible (P_1) and less-susceptible (P_2) bacteria. The model also included ATM degradation due to β-lactamases and its inhibition by AVI. ATM, aztreonam; AVI, avibactam.

Bacterial population was divided into two subpopulations: P_1 (responding to changes in ATM and AVI concentrations) and P_2 (less susceptible to ATM and not responding to AVI). The proportion of P_2 in the initial inoculum experimentally determined for each strain was used to define the initial conditions of P_1 and P_2 (P_2 fraction; **Table 2**). At the start of the experiment, the majority of bacteria was in the susceptible state with P_2 being around $1/10^5$ – $1/10^7$ of P_1. Moreover, differently from the reference model,[4] both subpopulations were actively growing at the same growth rate (K_{growth}, **Table 2 and Figure 3**), because the estimation of two different parameters for P_1 and P_2 resulted in very close values and a nonsignificant decrease in the objective function value given by NONMEM. No conversion between bacteria subpopulation was assumed.

ATM bactericidal activity was characterized by a sigmoidal maximum effect (E_{max}) model, and AVI enhancing effect was modeled as a decrease of ATM half-maximal effective concentration (EC_{50}) with increasing AVI concentrations using a bi-exponential function,[4] except for *E. coli* 1266865 for which a mono-exponential function better described the interaction between AVI concentration and ATM EC_{50}. The ATM-AVI interaction can be evaluated based on α and β values. At the same AVI concentrations, high α and β values result in an important decrease in ATM EC_{50} and, thus, an increase in ATM potency. Between the strains investigated, *E. coli* 1266865 showed the lowest α value (α = 0.42 L/mg), meaning that higher AVI concentrations are necessary to observe the same decay in ATM EC_{50} as for the other strains (α = 25.9–42.3 L/mg). In the present model, the ratio between EC_{50} values for the P1 and P2 subpopulations was referred as resistance factor and was ranging between 8 and 29, depending on the strains (**Table 2**).

Another sigmoidal E_{max} model was used to describe the bactericidal activity of AVI observed in all strains. For *E. coli* 1266865 and *E. cloacae* 1318536, large values were predicted for the Hill coefficient (φ = 12.9 and 8.91, respectively), and consequently, AVI effect could be described as an all-or-none response. Thus, no AVI bactericidal activity was observed at concentrations lower than the predicted EC_{50} and, at levels above the EC_{50}, AVI showed almost maximum bactericidal activity (**Figures 1 and 2, top panels b**). No AVI effect was assumed on the P_2 subpopulation because the EC_{50} values predicted by the model were much greater than the highest AVI concentrations used in the time-kill studies (32–64 mg/L) and were estimated with low precision.

Like in the reference model, ATM degradation rate was proportional to ATM concentration and depended on bacterial counts (P_1 + P_2). Different models were investigated to describe ATM degradation, and the selection of a model was based on the objective function value and graphical analysis (goodness-of-fit graphics). In the present model, the bacterial counts impacted on ATM degradation according to an exponential function instead of an E_{max} model. The prevention of degradation by AVI was modeled according to a fractional inhibitory E_{max} model, as described elsewhere.[5,8] Very low AVI concentrations were sufficient to prevent ATM degradation, as shown by the low estimated IC_{50} values (**Table 2**). Drug degradation model was not incorporated for the *E. coli* 1266865 strain because none was observed (**Figure 1, bottom panels**).

Simulations

The final model was used to simulate bacterial counts and ATM concentrations over time by taking into account ATM bactericidal effect and each of the three different effects of AVI separately against the four investigated strains. The individual contribution of each AVI effect during simulated static time-kill studies is shown in representative **Figures 4 and 5** for *E. coli* 1266865 and *E. cloacae* 1285905. The result of the

Table 2 Parameter estimates for the PD model based on four *Enterobacteriaceae* strains static time-kill kinetics and ATM degradation

Parameter	Description	Estimate (RSE%)			
		***Escherichia coli* 1266865**	***Citrobacter freundii* 974673**	***Enterobacter cloacae* 1285905**	***Enterobacter cloacae* 1318536**
Structural model					
N_{max} (log_{10} cfu/mL)	Maximum bacterial population size supported by the system	8.44 (0.27)	8.44 (0.27)	8.44 (0.27)	8.44 (0.27)
INOC (log_{10} cfu/mL)	Bacterial count at $t = 0$	6.01 (0.39)	6.01 (0.39)	6.01 (0.39)	6.01 (0.39)
P_2 fraction	Fraction of less sensitive subpopulation (P_2) present at $t = 0$	0.00001 fix	0.00001 fix	0.00002 fix	0.0000001 fix
K_{growth} (h^{-1})	Bacterial growth rate constant	0.907 (5.43)	1.1 (3.64)	1.15 (2.86)	1.24 (1.23)
$E_{max,ATM}$ (h^{-1})	Maximum kill rate constant associated to ATM	2.62 (5.1)	1.76 (3.1)	1.6 (2.3)	1.86 (1.7)
A (mg/L)	First parameter of bi-exponential function to characterize ATM EC_{50} in monotherapy	31.8 (11.5)	99.1 (6.8)	2.94 (7.7)	67.9 (3.3)
B (mg/L)	Second parameter of bi-exponential function to characterize ATM EC_{50} in monotherapy	0 fix	0.494 (6.5)	0.241 (6.7)	0.402 (5.7)
α (L/mg)	Exponential constant associated with A parameter that describes the relationship between AVI concentration and ATM potency	0.42 (1.5)	37.2 (1.2)	25.9 (3.1)	42.3 (2.8)
β (L/mg)	Exponential constant associated with B parameter that describes the relationship between AVI concentration and ATM potency	0 fix	0.548 (1.8)	0.602 (3.4)	0.412 (5.8)
γ	Hill coefficient that determined the steepness of the slope of the sigmoidal E_{max} curve associated with ATM bactericidal effect	1.48 (8.1)	1.42 (5.6)	2.65 (7.0)	1.52 (3.7)
Resistance factor	EC_{50} increasing factor for the less sensitive subpopulation	8.09 (5.7)	9.39 (4.2)	18 (7.2)	29.1 (4.2)
$E_{max,AVI}$ (h^{-1})	Maximum kill rate constant associated to AVI	2.28 (2.0)	1.29 (7.1)	1.69 (7.0)	2.14 (4.3)
$EC_{50,AVI}$ (mg/L)	Concentration of AVI that achieves half of the maximum kill rate for P_1	14.5 (2.8)	17.3 (6.8)	14.8 (14.7)	12 (5.1)
φ	Hill coefficient that described the steepness of the slope of the sigmoidal E_{max} curve associated with AVI bactericidal effect	12.9 (29.5)	4.63 (15.1)	2.1 (15.3)	8.91 (22.9)
Deg_{min} (h^{-1})	Minimum degradation rate constant of ATM	–	0.00462 (8.9)	0.000129 (2.9)	0.000166 (2.7)
ψ (mL/cfu)	Exponential constant associated with Deg_{min} that describes the relationship between the bacterial density ($P_1 + P_2$) and ATM degradation	–	0.563 (2.2)	1 fix	1 fix
IC_{50} (mg/L)	AVI concentration corresponding to a 50% decrease in ATM degradation rate	–	0.0000213 (48.4)	0.000185 (22.0)	0.0128 (8.3)
ϕ	Hill coefficient that described the steepness of the slope of the sigmoidal E_{max} model for inhibition of ATM degradation by AVI	–	0.207 (6.5)	0.522 (6.9)	1.48 (5.9)
Residual variability					
Additive error for bacterial counts (log_{10} cfu/mL)	Additive residual error that accounts to the difference between the observed values and model-predicted values for bacterial counts	0.97 (2.8)	0.708 (2.2)	0.845 (2.8)	0.782 (2.1)
Proportional error for ATM concentrations (%)	Proportional residual error that accounts to the difference between the observed values and model-predicted values for ATM concentration	10.1 (3.8)	49.4 (3.6)	24.4 (4.1)	33.3 (3.4)

ATM, aztreonam; EC_{50}, half-maximal effective concentration; E_{max}, maximum effect; PD, pharmacodynamic; RSE, Relative standard error.

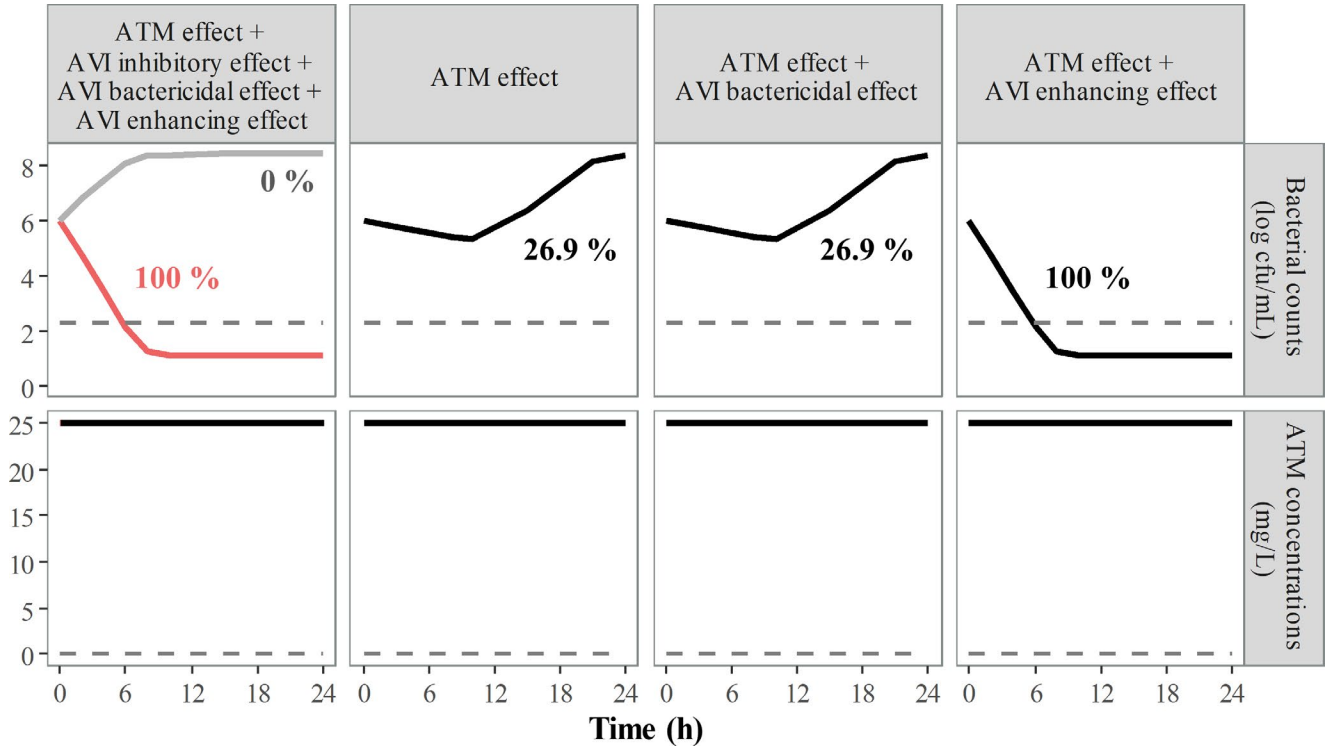

Figure 4 Simulations of the different effects of AVI on bacterial counts (top panels) in response to constant concentrations of 25–4.5 mg/L ATM-AVI in *Escherichia coli* 1266865, for which no ATM degradation was observed (bottom panels). Dashed lines correspond to the limit of quantification. Grey curve represents the control (0% effect) and red curve the maximum effect in bacterial killing (100%) predicted when all effects (ATM effect + the three AVI effects) are taken into account. The percentage of the maximum effect induced by ATM and each AVI effect is indicated for each simulated profile. ATM, aztreonam; AVI, avibactam.

simulations for *C. freundii* 974673 and *E. cloacae* 1318536 can be found in **Figure S5**. For all strains investigated, at a constant concentration of 25 mg/L of ATM and 4.5 mg/L of AVI, simulations based on the full model (i.e., with all effects taken into account) predicted bacterial killing, representing maximum effect of the combination, and no ATM degradation. The inhibitory effect of 4.5 mg/L AVI was predicted to prevent ATM degradation whatever the strain. However, this inhibitory effect did not prevent bacterial growth and resulted in a percentage of maximum effect close to that obtained with ATM alone (between 1.9% and 28.7% depending on the strain). When only ATM + AVI bactericidal effects were considered, bacterial growth was also predicted for all strains. According to the simulations, the effect that explained the combination efficacy was AVI enhancing effect, which by itself yielded a similar bacterial killing to the one obtained with the full model (around 100% of the maximum effect).

The different effects of AVI were also assessed at low and high ATM (5 and 125 mg/L, respectively) and AVI (0.9 and 22.5 mg/L, respectively) concentrations, that can be obtained in clinical practice when dosed every 8 hours at 2 *g* and 0.5 *g*, respectively (**Figures S6 and S7**). At low AVI levels, a bactericidal effect similar to that predicted with the full model was solely simulated with the AVI enhancing effect (between 82.5% and 100% of maximum effect), as it was observed at average concentrations. At high concentrations, AVI enhancing effect remained predominant for three of four strains, but the bactericidal effects of ATM and AVI also contributed to total effect (up to 99.3% for *E. cloacae* 1285905). Whatever the strain, the inhibitory effect of AVI poorly contributed to total effect (ATM effect + AVI inhibitory effect resulted in bacterial response similar to that for ATM alone with prediction of the corresponding AUC_{CFU} very close).

DISCUSSION

Drug interactions can be complex, and a more complete understanding of the pharmacokinetic-PD relationship of both drugs is crucial for optimizing drug combination dosing regimens.[13] Semimechanistic PD models are promising tools to quantify drug interactions, and, in this context, a PD model previously developed for ATM-AVI combination[4] could be extended for the four additional MDR *Enterobacteriaceae* evaluated in this study. The strains were chosen due to their various levels of resistance to ATM (MICs ranging from 32–512 mg/L), β-lactamase profiles—all strains producing diverse β-lactamases, including MBLs, such as NDM-1 and NDM-5—and for being of different species from those previously studied.

According to Sy *et al.*,[4] a phenomenon of heteroresistance was observed. However, to better characterize our data, slight modifications were made on the original model: both subpopulations were assumed to grow actively and ATM to exhibit bactericidal effect also on the less-susceptible subpopulation with a higher EC_{50}. In doing this, there

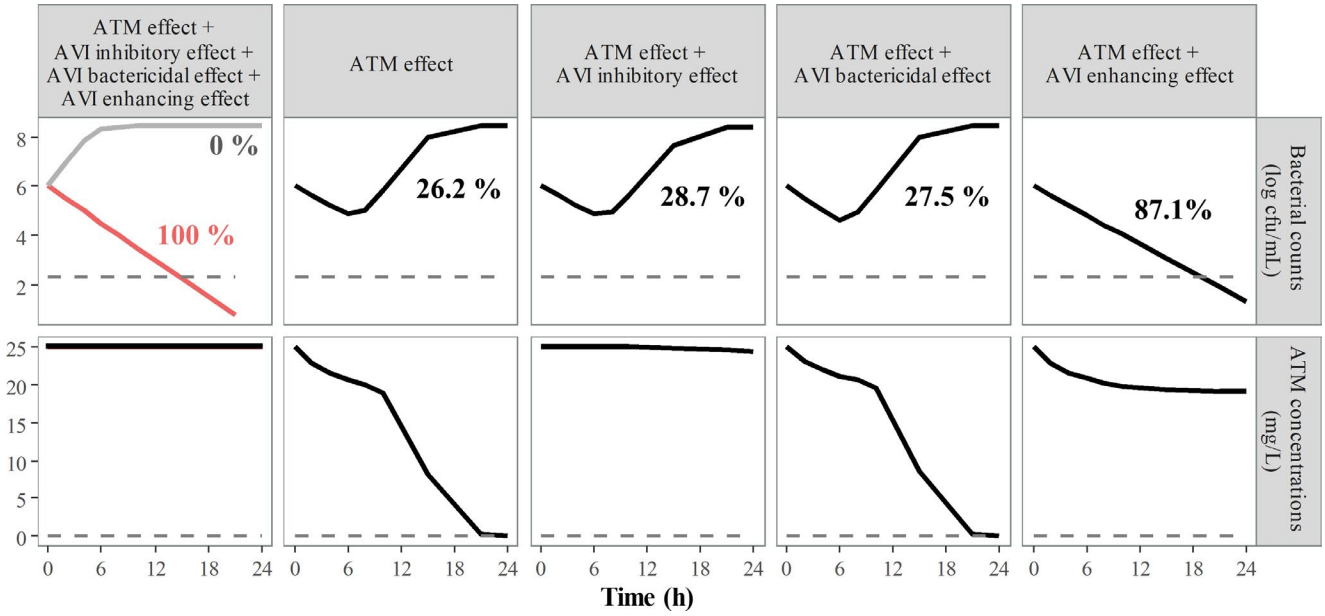

Figure 5 Simulations of the different effects of AVI on bacterial counts (top panels) and ATM degradation (bottom panels) in *Enterobacter cloacae* 1285905 in response to constant concentrations of 25–4.5 mg/L ATM-AVI. Dashed lines correspond to the limit of quantification. Grey curve represents the control (0% effect) and red curve the maximum effect in bacterial killing (100%) predicted when all effects (ATM effect + the three AVI effects) are taken into account. The percentage of the maximum effect induced by ATM and each AVI effect is indicated for each simulated profile. ATM, aztreonam; AVI, avibactam.

was no need for a delay function to explain regrowth. In our model, the proportion of P2 varied over time because this subpopulation was less susceptible to ATM-AVI and observed regrowth corresponded to P2. However, this P2 subpopulation was not microbiologically characterized, and it is not clear if this subpopulation was stable with time or if some other mechanisms of resistance developed over time (e.g., persisters). Moreover, ATM degradation was modeled according to an exponential function instead of an E_{max} model, and the prevention of ATM degradation was related to AVI concentrations. In our study, this could be explained by the fact that lower AVI concentrations were used in combination and not only high AVI levels that could prevent the whole degradation. In this way, the relationship between AVI levels and the degree of ATM degradation could be characterized as performed for ceftazidime-avibactam.[5]

β-Lactamase inhibition by AVI was evaluated indirectly by monitoring the time course of ATM concentrations in the presence and absence of AVI. Similar to what was reported by Sy et al.,[12] in the absence of AVI, no ATM degradation was observed in the time-kill study for the *E. coli* isolate, despite the differences between β-lactamases expressed by these isolates (**Figure 1, bottom panels**). As expected, for the other strains, AVI could prevent ATM degradation even at very low concentrations consistent with its very high efficacy.[2]

Surprisingly, although AVI efficiently prevented ATM degradation by β-lactamases, our model suggested that this effect was not the most important to explain bacterial killing. In fact, at an average concentration of ATM of 25 mg/L, when only AVI inhibitory effect was taken into account and ATM degradation was totally prevented for most strains, ATM concentrations were not high enough to yield bacterial killing, producing no more than 30% of maximum effect (**Figure 5**). Indeed, ATM concentrations were still lower than EC_{50} of ATM in monotherapy (EC_{50} either for the susceptible or less-susceptible subpopulation). Therefore, keeping ATM concentrations stable thanks to β-lactamases inhibition was not sufficient to explain bacterial killing observed when ATM was combined with AVI.

Besides the β-lactamase inhibitory effect, AVI shows intrinsic bactericidal activity at higher concentrations[14] due to inhibition of PBP2.[3] MIC values for AVI alone were around 16–32 mg/L for the four *Enterobacteriaceae* studied, consistent with previously reported values for others isolates.[3,14,15] This effect affected bacterial counts only at high concentration (22.5 mg/L), which suggests that in clinical practice it would be marginal because concentrations will rapidly decrease due to the short half-lives of both compounds (terminal half-life ATM = terminal half-life AVI = 2 hours).[10,16]

As described for other β-lactamase inhibitors belonging to the DBO class, a third effect could be characterized for AVI, which is the capability to enhance ATM activity. Although AVI is not considered a potent β-lactam enhancer,[2,17] this effect was shown to be the most important to achieve full bacterial eradication, according to the simulations performed in the present study (around 100% of maximum effect; **Figures 4 and 5**). The enhancement of the activity of ATM by AVI occurs due to the simultaneous binding to different PBPs in the bacterial membrane.[2,18] ATM targets PBP3,[19] whereas AVI binds to PBP2.[3] Similar findings were observed when AVI was combined with ceftazidime,[5] a β-lactam that also targets PBP3.[20] This AVI mechanism of action, successfully implemented in the model, confirms the recent results from Sutaria *et al.*[18] suggesting that when combining two β-lactams, or a β-lactam

with a β-lactamase inhibitor that has affinity for PBPs, it is important to consider their respective affinity for PBPs and the relative expression of PBPs. Differently to what was observed for AVI combined with ceftazidime against an *E. coli* strain,[2] the enhancing effect could be observed even at low and clinically attainable concentrations (**Figure S6**). This enhancing effect was characterized in the model by a dramatic decrease of ATM EC_{50} in the presence of clinically achievable AVI concentrations, restoring the susceptibility of the four different strains to ATM. This effect can be particularly apprehended with the *E. coli* strain, for which no hydrolysis of ATM was observed but whose ATM MIC decreased from 32 to 4 mg/L in the presence of 4 mg/L of AVI. Moreover, it should be noted that by enhancing ATM efficacy, this effect decreased bacterial counts and, thus, reduced ATM hydrolysis by β-lactamases (**Figure 5**).

Knowing that AVI has three distinct effects—β-lactamases inhibition, bactericidal activity, and enhancement of ATM activity—and the last one being the major contributor for the final combined effect, at least during time-kill studies, dosing regimens should be optimized in order to achieve the maximum interaction. Today, the majority of dosing regimens for β-lactam/β-lactamase inhibitor combinations are chosen assuming that the only effect of the β-lactamase inhibitor is to prevent β-lactam degradation, and, thus, the combination is chosen mainly based on the β-lactamases expressed by pathogens. The findings of the present study suggest that β-lactamase inhibitors belonging to the DBO class should rather be chosen based on their pharmacological synergy with the β-lactam, and particularly, as suggested by Sutaria *et al*.,[18] on their respective affinity for PBPs.

Nevertheless, this study has its limitations. The model and simulations were derived from static time-kill experiments and could, therefore, characterize the relative contribution of the various mechanism of action to the overall antimicrobial effect, at least during the early stage of treatment, because a time effect on ATM-AVI PDs may not be excluded. Therefore, complementary *in vitro* (hollow-fiber) and even *in vivo* experiments (using murine infection models) should be necessary before using this PD model to evaluate the contribution of each AVI effect in the clinical setting. Moreover, a small number of strains was included in this study due to the time and resources required for time-kill studies with drug combinations, and, thus, no inter-strain variability was implemented in the model. More strains should be investigated to well characterize such variability, identify relevant covariates, and predict responses for other isolates not studied. It is also important to keep in mind that semimechanistic models are simplifications of the biological processes and do not predict with accuracy what will occur in patients but still are informative tools that enable the integration of all available data to explore the complex interaction between drug combinations.

In conclusion, clinical concentrations of ATM and AVI showed efficacy *in vitro* against MDR *Enterobacteriaceae* producing MBLs, and the semimechanistic PD model could well characterize the three previously reported effects of AVI. On top of that, in the present study, the individual contribution of each AVI effect to the combined activity with ATM was evaluated. Within the clinical range of ATM-AVI concentrations, even though AVI demonstrated high efficiency to prevent ATM hydrolysis, the combined bactericidal activity was mostly explained by AVI enhancing effect. This suggests that, in the choice of a β-lactam/β-lactamase inhibitor combination, the synergy between the β-lactamase inhibitor and the β-lactam should also be considered in addition to the spectrum of β-lactamases covered by the β-lactamase inhibitor.

Supporting Information. Supplementary information accompanies this paper on the *CPT: Pharmacometrics & Systems Pharmacology* website (www.psp-journal.com).

Figure S1. Model-prediction and observed static-time kill curves of ATM and AVI against *E. coli* 1266865 over 27 hours (top panels) and the percentage of the initial ATM concentration remaining in the system during the time-kill experiments (bottom panels).
Figure S2. Model-prediction and observed static-time kill curves of ATM and AVI against *C. freundii* 974673 over 27 hours (top panels) and the percentage of the initial ATM concentration remaining in the system during the time-kill experiments (bottom panels).
Figure S3. Model-prediction and observed static-time kill curves of ATM and AVI against *E. cloacae* 1285905 over 27 hours (top panels) and the percentage of the initial ATM concentration remaining in the system during the time-kill experiments (bottom panels).
Figure S4. Model-prediction and observed static-time kill curves of ATM and AVI against *E. cloacae* 1318536 over 27 hours (top panels) and the percentage of the initial ATM concentration remaining in the system during the time-kill experiments (bottom panels).
Figure S5. Simulations of the different effects of AVI on bacterial counts in response to constant concentrations of 25–4.5 mg/L ATM-AVI in four *Enterobacteriaceae* strains.
Figure S6. Simulations of the different effects of AVI on bacterial counts in response to constant concentrations of 5–0.9 mg/L ATM-AVI in four *Enterobacteriaceae* strains.
Figure S7. Simulations of the different effects of AVI on bacterial counts in response to constant concentrations of 125–22.5 mg/L ATM-AVI in four *Enterobacteriaceae* strains.
Supplementary Material S1. Contains drug stability analysis, a detailed explanation of the *in vitro* PD model, the procedure of how the full model was reduced to conduct simulations and the model code.

Acknowledgments. Part of this research was presented at the 28th European Society of Clinical Microbiology and Infectious Diseases, April 21–24, 2018, Madrid, Spain. We thank France Mentré for her helpful discussion on the modeling and Emma Marquizeau for her technical assistance with the time-kill curve experiments.

Funding. This research project was funded by the Innovative Medicine Initiative Joint undertaking under COMBACTE-CARE grant agreement 115620 resources of which are composed of financial contributions from the European Union Seventh Framework Programme (FP7/2007–2013) and European Federation of Pharmaceutical Industries and Associations (EFPIA) companies in kind contribution. Avibactam dry powder was provided by Pfizer.

Conflict of Interest. B. J. is currently an employee of Pfizer. All other authors declared no competing interests for this work.

Author Contributions. A.C., B.G.S.T., B.J., W.C., and N.G. wrote the manuscript. A.C., B.G.S.T., J.B., B.J., S.M., W.C., and N.G. designed

the research. A.C., B.G.S.T., and C.A. performed the research. A.C., B.G.S.T., and N.G. analyzed the data.

1. Biedenbach, D.J., Kazmierczak, K., Bouchillon, S.K., Sahm, D.F. & Bradford, P.A. In vitro activity of aztreonam-avibactam against a global collection of gram-negative pathogens from 2012 and 2013. *Antimicrob. Agents Chemother.* **59**, 4239–4248 (2015).
2. Morinaka, A. *et al.* OP0595, a new diazabicyclooctane: mode of action as a serine beta-lactamase inhibitor, antibiotic and beta-lactam 'enhancer'. *J. Antimicrob. Chemother.* **70**, 2779–2786 (2015).
3. Asli, A., Brouillette, E., Krause, K.M., Nichols, W.W. & Malouin, F. Distinctive binding of avibactam to penicillin-binding proteins of gram-negative and gram-positive bacteria. *Antimicrob. Agents Chemother.* **60**, 752–756 (2016).
4. Sy, S. *et al.* Prediction of in vivo and in vitro infection model results using a semimechanistic model of avibactam and aztreonam combination against multidrug resistant organisms. *CPT Pharmacometrics Syst. Pharmacol.* **6**, 197–207 (2017). https://doi.org/10.1002/psp4.12159
5. Sy, S.K.B. *et al.* A mathematical model-based analysis of the time-kill kinetics of ceftazidime/avibactam against Pseudomonas aeruginosa. *J. Antimicrob. Chemother.* **73**, 1295–1304 (2018).
6. Wang, D.Y., Abboud, M.I., Markoulides, M.S., Brem, J. & Schofield, C.J. The road to avibactam: the first clinically useful non-beta-lactam working somewhat like a beta-lactam. *Future Med. Chem.* **8**, 1063–1084 (2016).
7. European Committee for Antimicrobial Susceptibility Testing (EUCAST) of the European Society for Clinical Microbiology and Infectious Diseases (ESCMID) EUCAST Discussion Document E. Dis 5.1: determination of minimum inhibitory concentrations (MICs) of antibacterial agents by broth dilution. *Clin. Microbiol. Infect.* **9**, 1–7 (2003).
8. Sy, S.K.B. & Derendorf, H. Experimental design and modelling approach to evaluate efficacy of beta-lactam/beta-lactamase inhibitor combinations. *Clin. Microbiol. Infect.* **24**, 707–715 (2018).
9. Vinks, A.A., van Rossem, R.N., Mathot, R.A., Heijerman, H.G. & Mouton, J.W. Pharmacokinetics of aztreonam in healthy subjects and patients with cystic fibrosis and evaluation of dose-exposure relationships using Monte Carlo simulation. *Antimicrob. Agents Chemother.* **51**, 3049–3055 (2007).
10. Merdjan, H., Rangaraju, M. & Tarral, A. Safety and pharmacokinetics of single and multiple ascending doses of avibactam alone and in combination with ceftazidime in healthy male volunteers: results of two randomized, placebo-controlled studies. *Clin. Drug Investig.* **35**, 307–317 (2015).
11. The European committee on antimicrobial susceptibility testing (EUCAST) (2018). Breakpoint tables for interpretation of MICs and zone diameters, version 8.0.
12. Sy, S.K. *et al.* In vitro pharmacokinetics/pharmacodynamics of the combination of avibactam and aztreonam against MDR organisms. *J. Antimicrob. Chemother.* **71**, 1866–1880 (2016).
13. Brill, M.J.E., Kristoffersson, A.N., Zhao, C., Nielsen, E.I. & Friberg, L.E. Semi-mechanistic pharmacokinetic-pharmacodynamic modelling of antibiotic drug combinations. *Clin. Microbiol. Infect.* **24**, 697–706 (2018).
14. Lagace-Wiens, P.R. *et al.* Activity of NXL104 in combination with beta-lactams against genetically characterized Escherichia coli and Klebsiella pneumoniae isolates producing class A extended-spectrum beta-lactamases and class C beta-lactamases. *Antimicrob. Agents Chemother.* **55**, 2434–2437 (2011).
15. Berkhout, J., Melchers, M.J., van Mil, A.C., Nichols, W.W. & Mouton, J.W. In vitro activity of ceftazidime-avibactam combination in in vitro checkerboard assays. *Antimicrob. Agents Chemother.* **59**, 1138–1144 (2015).
16. Ramsey, C. & MacGowan, A.P. A review of the pharmacokinetics and pharmacodynamics of aztreonam. *J. Antimicrob. Chemother.* **71**, 2704–2712 (2016).
17. Livermore, D.M., Warner, M., Mushtaq, S. & Woodford, N. Interactions of OP0595, a novel triple-action diazabicyclooctane, with beta-lactams against OP0595-resistant Enterobacteriaceae mutants. *Antimicrob. Agents Chemother.* **60**, 554–560 (2016).
18. Sutaria, D.S. *et al.* First penicillin-binding protein occupancy patterns of beta-lactams and beta-lactamase inhibitors in Klebsiella pneumoniae. *Antimicrob. Agents Chemother.* **62**, pii: e00282-18 (2018).
19. Georgopapadakou, N.H., Smith, S.A. & Sykes, R.B. Mode of action of azthreonam. *Antimicrob. Agents Chemother.* **21**, 950–956 (1982).
20. Hayes, M.V. & Orr, D.C. Mode of action of ceftazidime: affinity for the penicillin-binding proteins of Escherichia coli K12, Pseudomonas aeruginosa and Staphylococcus aureus. *J. Antimicrob. Chemother.* **12**, 119–126 (1983).